Supporting Information for

Thermodynamical Stable Synthesis of High Entropy Alloy and Efficiently Catalyzed Oxidation of 5-Hydroxymethylfurfural into 2,5-Furandicarboxylic acid in Base-free Condition

Guangqiang Lv, [a*] Shan Liu, [a] Xiaoyan Chen, [a] Mengxin Chen, [a] Yanjuan Wu, [a] Yuji Gao, [a] Shuai Wang, [a] Furong Tao, [a] Jingui Wang, [a*] Liwei Niu [a*]

[a] School of Chemistry and Chemical Engineering, Qilu University of Technology (Shandong Academy of Sciences), Jinan 250353, Shandong, China. E-mail: lvguangqiang@qlu.edu.cn JGWang@qlu.edu.cn; niuliwei@qlu.edu.cn

1. **Materials and Catalysts Preparation**
2. **Catalytic performance test of catalysts**
3. **Catalyst characterizations**
4. **ICP analysis of prepared HEA/C**
5. **CO_2-TPD test of various HEA/C comparison with active carbon**
6. **XPS characterization of prepared Fe1Co1Ni1Cu1Ga1Pt2/C**
7. **Morphology and composition between recycled and freshly prepared Fe1Co1Ni1Cu1Ga1Pt2/C**
8. **TOF value comparison between various catalyst**
9. **FDCA productivity comparison between various catalysts**
10. **DFT study**

1. Materials and Catalysts Preparation

Materials. $Fe(NO_3)_3 \cdot 9H_2O$ (Sinopharm chemical)、$Co(NO_3)_2 \cdot 6H_2O$ (Sinopharm chemical)、$Ni(NO_3)_2 \cdot 6H_2O$ (Sinopharm chemical)、$Cu(NO_3)_2 \cdot 3H_2O$ (Sinopharm chemical)、$H_2PtCl_6 \cdot 6H_2O$ （Aladdin）、sodium borohydride (Aladdin)、Gallium metal (Aladdin)、methanol, ethanol (Tianjin Fuyu Chemical), 5-hydroxymethylfurfural, 2, 5-diformylfuran, 2-formyl-5-furanoic acid (Aladdin), 2,5-furandicarboxylic acid (J&K Scientific). deionized water, (18 MΩ cm)

Preparation of 1 wt.% Ga/C

Procedure of HEA/C synthesis are according to literature and appropriate modification was made.[1-6] In the preparation of Ga/C, initially, metallic gallium is heated in a water bath to 40 °C to fully melt it into liquid gallium. Liquid gallium was taken by a spatula pre-soaked in 60 °C hot water to prevent it solidification upon cooling. 100 mg of liquid gallium and 650 μL of dodecanethiol was added into10 ml isopropanol. The mixture was then ultrasonic dispersion for 4 to 6 hours. The resultant dispersion is designated as Solution A.

1 g of activated carbon (AC) powder (200 mesh) was dispersed into a mixture containing 20 mL of deionized water and 20 ml of ethanol. The mixture is stirred at room temperature for 20 minutes. Subsequently, 1.065 mL of Solution A is added to the activated carbon suspension, followed by continuous stirring for 6 hours to ensure thorough and uniform adsorption of the metallic gallium onto AC. The mixture is then centrifuged at 10000 rpm for 15 minutes, and the resulting precipitate is washed three times with water and ethanol subsequently. The washed product is dried in at 25 °C for 4 hours, yielding a 1% wt.% Ga/C sample. The preparation of Ga/C samples with other mass loadings follows a similar procedure. It should be noted that during the drying process in the air-drying oven, the surface of the gallium nanoparticles oxidizes to gallium oxide, while the core remains as metallic gallium.

Preparation of 6 wt.% $Fe_1Co_1Ni_1Cu_1Ga_1Pt_1$/C

40.4 mg $Fe(NO_3)_3 \cdot 9H_2O$ (0.1 mmol), 29.1 mg $Co(NO_3)_2 \cdot 6H_2O$ (0.1 mmol), 29.1 mg $Ni(NO_3)_2 \cdot 6H_2O$ (0.1 mmol), 24.2 mg $Cu(NO_3)_2 \cdot 3H_2O$ (0.1 mmol), and 51.8 mg

$H_2PtCl_6 \cdot 6H_2O$ (0.1 mmol) (element molar ratio Fe:Co:Ni:Cu:Pt = 1:1:1:1:1) were dispersed in 60 mL deionized water and sonicated for 15 minutes to obtain a clear and homogeneous solution. Then, 700 mg of 1% Ga/C was added to the solution and stir for another 2 hours. The powder was separated in rotary evaporator and ground in an agate mortar before transferred into a ceramic boat. After that, the powder was calcinated at 650 °C for 6 hours under a flow of Ar/H_2 (95:5) at a rate of 25 mL/min. The resulting sample is denoted as $Fe_1Co_1Ni_1Cu_1Ga_1Pt_1/C$. The synthesis of other elemental ratio HEA/C catalysts follows a similar procedure.

2. Catalytic performance test of catalysts

In a typical experiment, 20 mL H_2O containing 1 mol HMF was added into a 100 mL stainless steel autoclave with a Teflon vessel liner. 200 mg as-prepared HEA/C catalyst was added into the reactor and 0.5 MPa oxygen was introduced into the reactor after the reactor was sealed. The reactant mixture was heated to desired temperature under vigorous stirring (800 rpm) and liquid samples were taken at pre-determined time interval and analyze as following method. In radical quenching experiment, 1 mmol HMF, 20 mL mixed methanol and water (with different ratio), 200 mg of catalyst were added into the reactor and 0.5 MPa oxygen was introduced into the reactor. The reactant mixture was heated to 100 ℃ and kept for 4 h before analysis the reaction mixture. In catalyst recycle tests, the catalyst was recovered by filtration and washed with 150 mL acetonitrile and water for three times (50 mL acetonitrile and water continuously in each rinse) and dried in oven at 105 ^oC overnight before next test.

HMF conversion and products yields were determined by high-performance liquid chromatography (HPLC, Aminex HPX-87H column from Bio-Rad Laboratories Co., Ltd., 0.5 mM H_2SO_4 aqueous solution as the eluent, 0.6 mL min^{-1} flow rate, at 35 ^oC). The products were identified by comparison with known commercially pure samples. The HMF conversion, products yields were calculated as following equations：

HMF conversion (mol. %) $=(1-\frac{n_{HMF}}{N_{HMF}}) \times 100\%$

Products Yield (mol.%) $=\frac{n_p}{N_{HMF}} \times 100\%$

Where: the n_{HMF} stands for HMF mole amount residues in reaction mixture;

the n_p stands for detected mole amount of products (it can be HMFCA, DFF, FFCA and FDCA) in reaction mixture;

the N_{HMF} stands for total HMF mole amount input the reactor in the beginning of reaction.

3. Catalyst characterizations

For the prepared catalyst, the powdered samples with grinding enough were used for the structure characterization. X-ray diffractometer (XRD) was produced by Bruker company in Germany, using Cu Kα radiation at 40 kV and 40 mA with a scanning speed (2θ) of 20 °/min. X-ray photoelectron spectroscopy (XPS) measurements were performed by a K-alpha XPS spectrometer using monochromatic Al Kα radiation generated from an electron beam operated at 15 kV and 32.3 W. Samples were collected under ultra-high vacuum (at 10^{-7} mbar) and room temperature at a pass energy of 50 eV to avoid sample charging. In order to compensate for the charging effect, all binding energies were referenced to the C 1s of 284.8 eV. The peak fitting was carried out by the Avantage (Thermo Scientific) software package. The material morphologies and microstructures were characterized by High resolution field emission transmission electron microscope (TEM) conducting on a JEM-2100F microscope operated at 1000 kV. High-resolution TEM images (HRTEM) and electron energy dispersive spectroscopy (EDS) mapping were taken on the same microscope. The atomic structural characterization of the samples was determined using an aberration-corrected FEI Titan Cubed Themis G2 microscope operated at 300 kV equipped with an X-FEG gun and Bruker Super-X EDX detectors. The beam current was ~50 pA, the convergence semi-angle was 30 mrad, and a collection semi-angle snap was 80-379 mrad. The STEM-EDX mapping are acquired at a beam current of ~50 pA and counts

ranging from 1k cps to 3k cps for ~15 min with a Bruker Super-X EDS four-detector. Due to the ultrasmall nanostructure, the electron exposures used should be very low to minimize irradiation damage during the TEM measurements. Various metal loading on each HEA/C was determined by Inductively Coupled Plasma Atomic Emission Spectrometry (ICP-AES) (Optima2100DV, PerkinElmer). CO_2-TPD characterization were carried out on ChemStar Chemical adsorption analyzer. Before sample testing, the sample was loaded into the test tube and dehydrated and degassed at 150°C for 2 hours. Subsequently, the sample was saturated with CO_2 gas for 1 hour at room temperature (using a mixture of 90% Ar and 10% CO_2 at a flow rate of 50 mL/min). The sample was then purged with Ar (50 mL/min) at room temperature for 10 minutes. After that, a temperature-programmed desorption (TPD) process was initiated, the sample was heated from room temperature to 900 ^oC at a heating rate of 5 ^oC/min while collecting TCD signals. When one test was finished, the sample was allowed to cool down to room temperature naturally.

4. ICP analysis of prepared HEA/C

Table S1. ICP test of prepared various HEA/C materials

HEA/C	Fe (wt.%)	Co (wt.%)	Ni (wt.%)	Cu (wt.%)	Pt (wt.%)	Ga (wt.%)	Total (wt.%)
$Fe_1Co_1Ni_1Cu_1Ga_1Pt_2/C$	0.54	0.66	0.68	0.67	3.51	0.67	6.73
$Fe_1Co_1Ni_1Cu_1Pt_1/C$	0.83	0.88	1.12	1.05	2.97	---	6.85
$Fe_1Co_1Ni_1Cu_1Ga_1Pt_1/C$	0.81	0.83	0.77	0.92	2.81	1.08	7.22
$Fe_1Co_1Ni_1Cu_1Ga_1/C$	1.31	1.38	1.44	1.36	---	1.42	6.91

5. CO_2-TPD test of various HEA/C comparison with active carbon

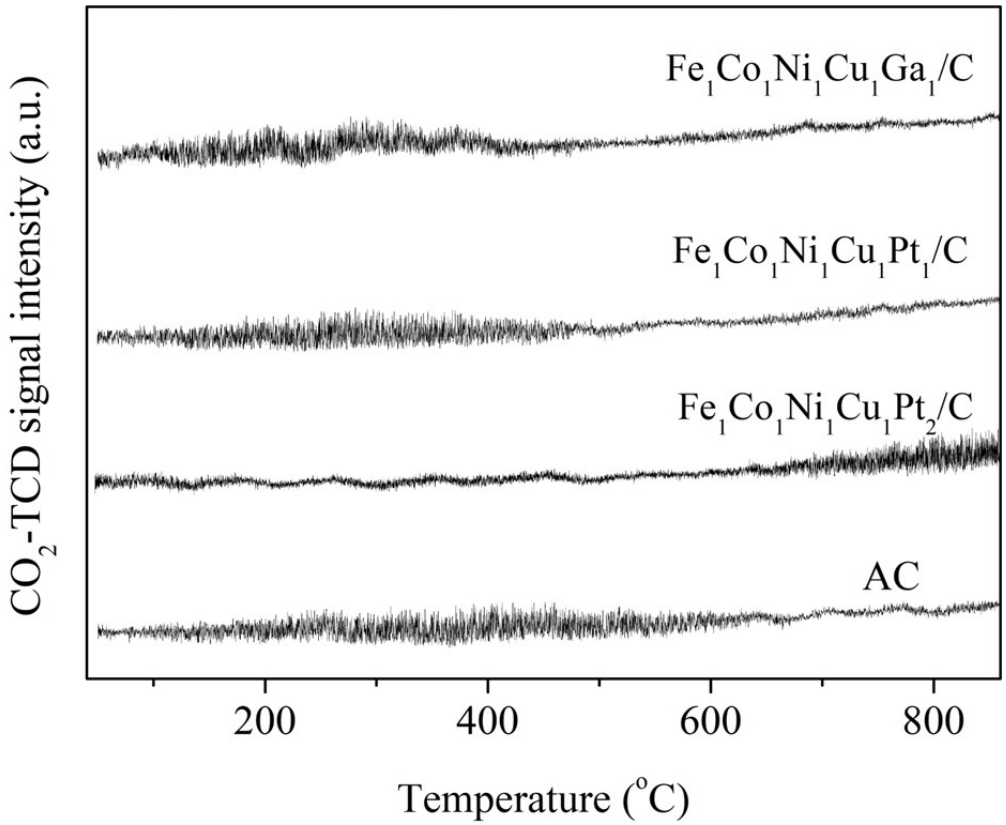

Figure S1. CO_2-TPD test of prepared HEA/C and comparison with active carbon

6. XPS characterization of prepared $Fe_1Co_1Ni_1Cu_1Ga_1Pt_2/C$

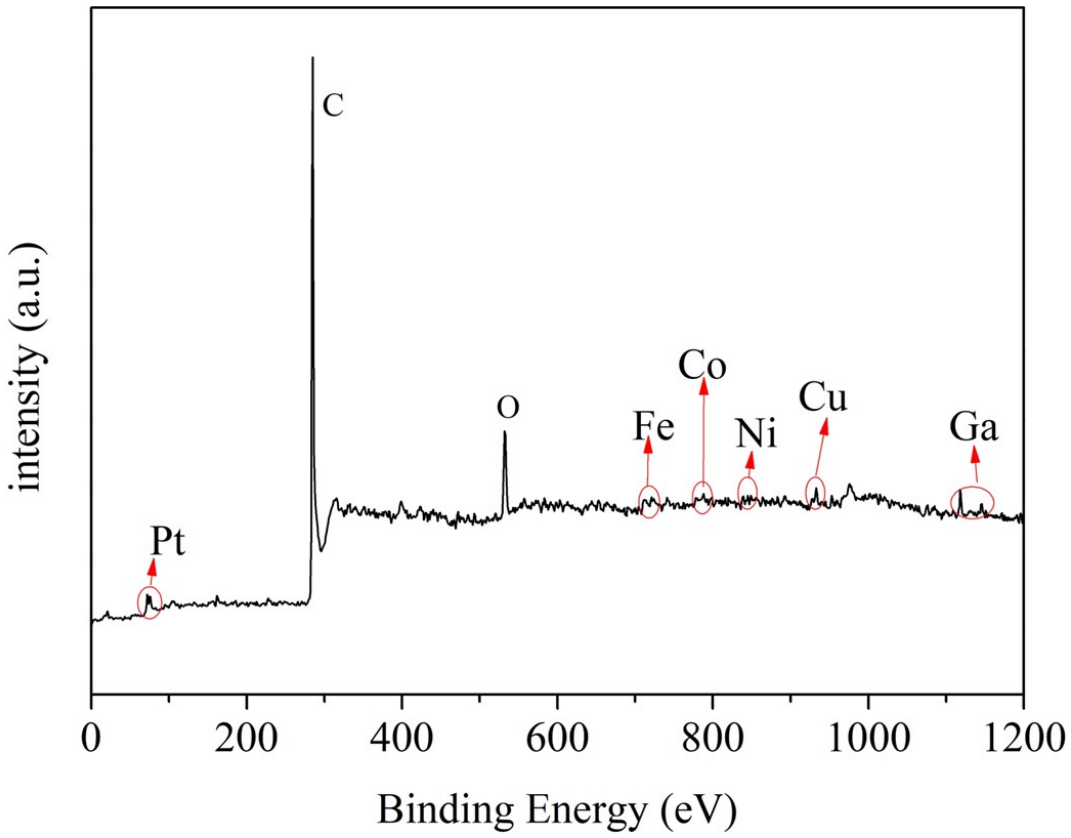

Figure S2. XPS survey spectrum of prepared HEA/C

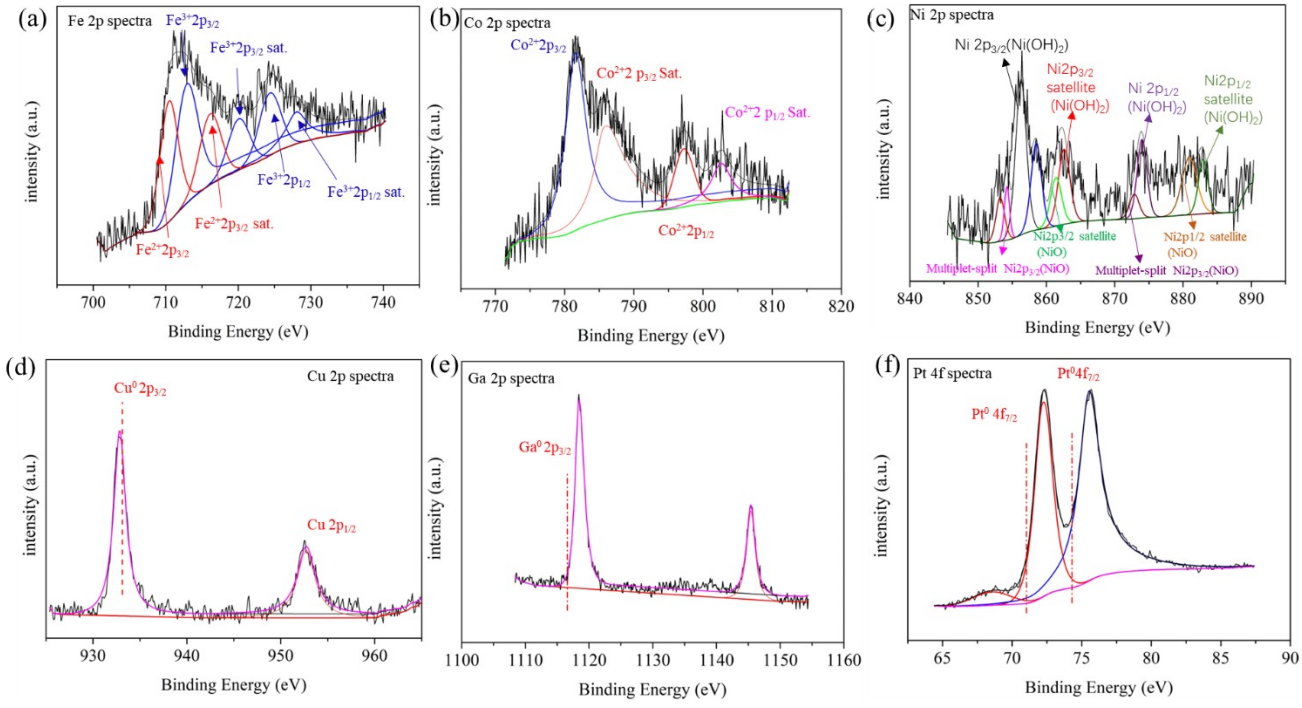

Figure S3. XPS spectra collected at the (a) Fe 2p, (b) Co 2p, (c) Ni 2p, (d) Cu 2p, (e) Ga 2p, (f) Pt 4f edges for the prepared $Fe_1Co_1Ni_1Cu_1Ga_1Pt_2/C$

7. Morphology and composition between recycled and freshly prepared $Fe_1Co_1Ni_1Cu_1Ga_1Pt_2/C$

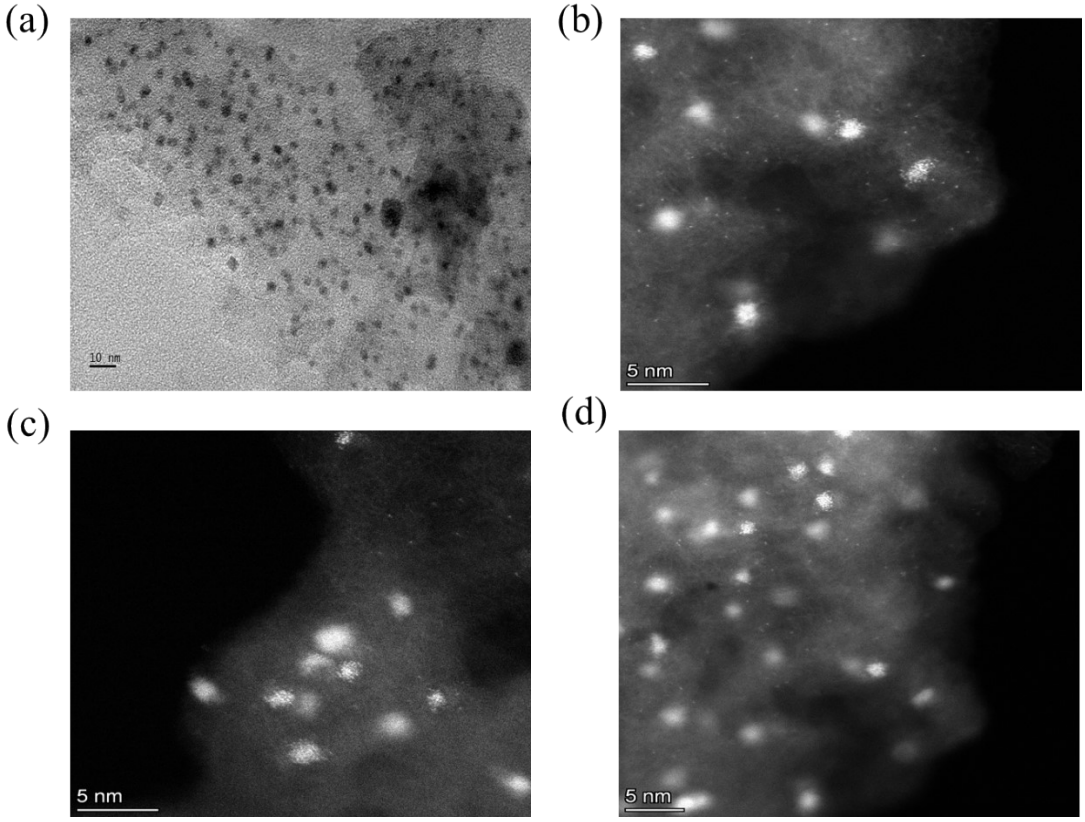

Figure S4. HRTEM images of recycled $Fe_1Co_1Ni_1Cu_1Ga_1Pt_2/C$ in catalyst recycle tests.

Table S2. ICP test of various metal elements in freshly prepared and recycled $Fe_1Co_1Ni_1Cu_1Ga_1Pt_2/C$

HEA/C	Fe (wt.%)	Co (wt.%)	Ni (wt.%)	Cu (wt.%)	Pt (wt.%)	Ga (wt.%)	Total (wt.%)
$Fe_1Co_1Ni_1Cu_1Ga_1Pt_2/C$-fresh	0.54	0.66	0.68	0.67	3.51	0.67	6.73
$Fe_1Co_1Ni_1Cu_1Ga_1Pt_2/C$-recycled	0.51	0.71	0.58	0.71	3.32	0.62	6.45

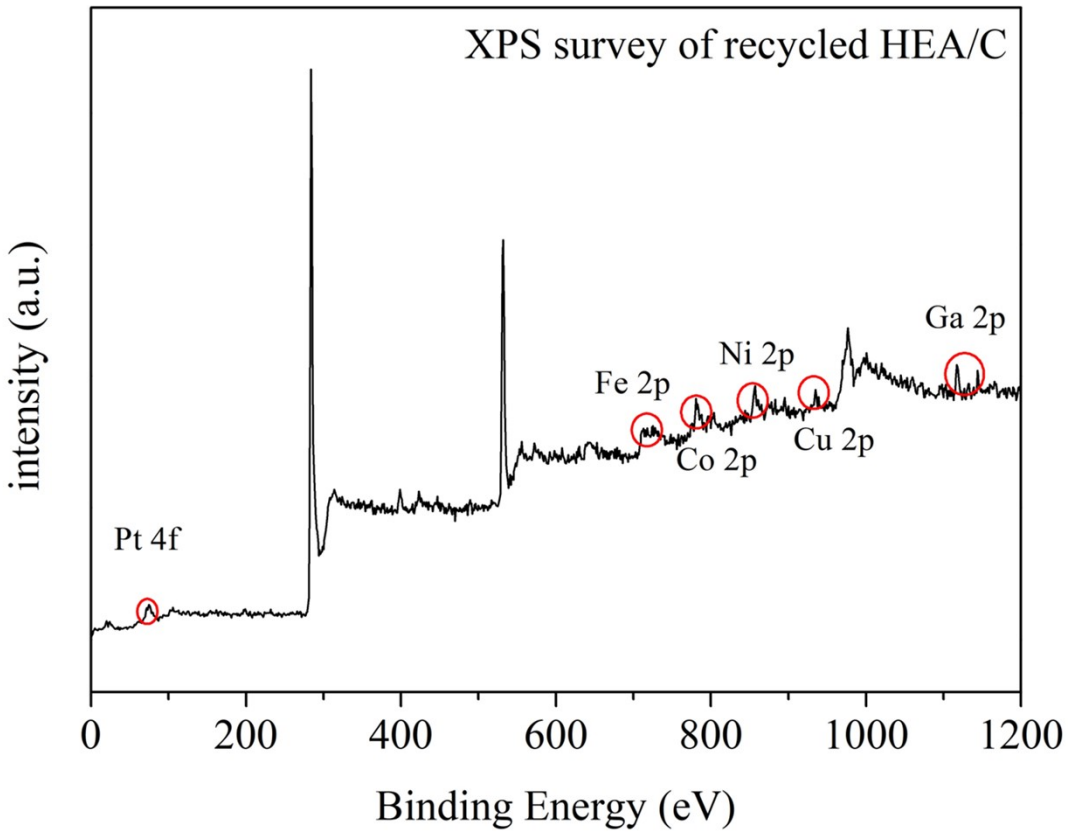

Figure S5. XPS spectrum of recycled $Fe_1Co_1Ni_1Cu_1Ga_1Pt_2/C$ in catalyst recycle tests.

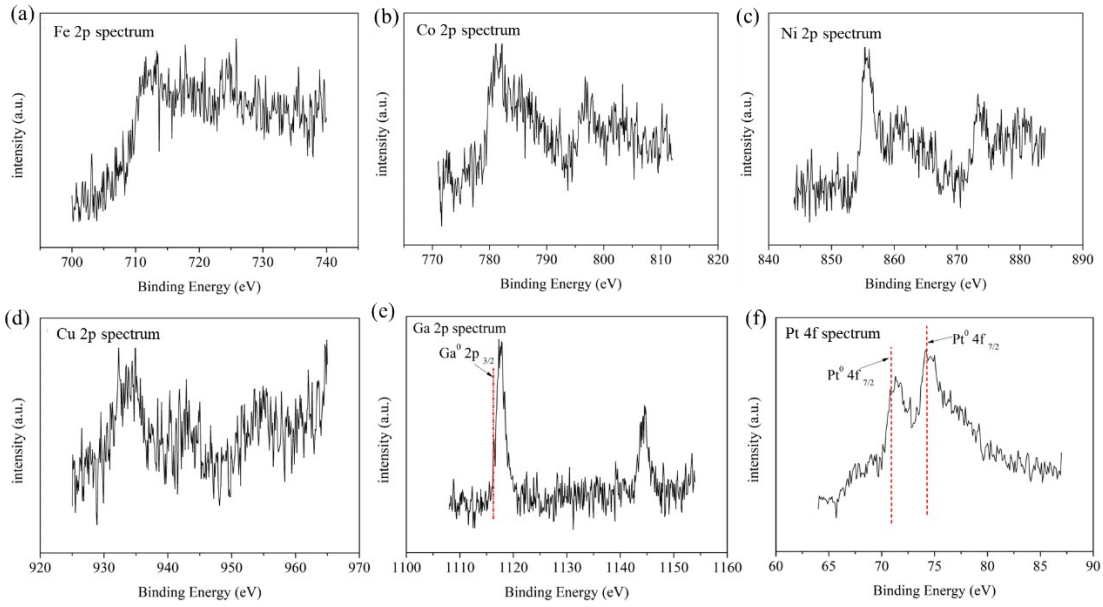

Figure S6. XPS spectra collected at the (a) Fe 2p, (b) Co 2p, (c) Ni 2p, (d) Cu 2p, (e) Ga 2p, (f) Pt 4f edges for recycled $Fe_1Co_1Ni_1Cu_1Ga_1Pt_2/C$ in catalyst recycle tests.

8. TOF value comparison between various catalysts

Table S3. Reported TOF values over various catalytic sites in literature

Entry	Catalyst	TOF	[Ref.]
1	NC-Cu/MgAlO	238.6 h^{-1}	7
2	Au_1-Pd_1@PECN	128.5 h^{-1}	8
3	Au NPs/CNT	109.3 h^{-1}	9
4	MnO_2	0.2 h^{-1}	10
5	$Ni_{0.90}Pd_{0.10}$	65.3 h^{-1}	11
6	CeCP@Pt (4.5nm)	0.177 s^{-1}	12
7	Au/HSAG	1195 h^{-1}	13
8	Pd/HPGS	62 h^{-1}	14
9	Au-Pd/ZOC	24 h^{-1}	15
10	Pt/CNT	0.91 s^{-1}	16
11	Au/CeO_2	12.9 h^{-1}	17
12	$1.5Au_3Cu_1$	14.5 h^{-1}	18
13	Au/C (WGC)	5.0 s^{-1}	19
14	$Fe_1Co_1Ni_1Cu_1Ga_1Pt_2$/C	52.9 h^{-1}	This work

9. FDCA productivity comparison between various catalysts

Table S4. Summary of FDCA yield and productivity for previous studies

Substrates	Catalyst-solvent system for FDCA production	Reaction conditions	Yield (%)	Productivity [mmol $g_{catalyst}^{-1}$ h^{-1}]	[Ref]
Fructose (0.18 g)	Au_8Pd_2/HT (0.25 g), Na_2CO_3 (0.106 g), water (10 mL)	95 °C, 20 h	78	0.156	**20**
Glucose (0.18 g)	Au_8Pd_2/HT (0.25 g), Na_2CO_3 (0.106 g), water (10 mL)	95 °C, 50 h	48	0.038	**20**
Sucrose (converted to 0.3 mmol HMF)	Au/ZrO_2 (98 mg), NaOH (2.5 M), water (10 mL)	125 °C, 20 h	29	0.044	**21**
Fructose (0.55 mmol)	Pd/CC (0.02 g), K_2CO_3 (0.23 g), water (5 mL)	140 °C, 30 h	64	0.587	**22**

Fructose (1 mmol)	Au/HT (0.25 g), water (10 mL), Na_2CO_3 (1 mmol)	95 °C ,7 h	83	0.474	**23**
Jerusalem artichoke (equiv. to 1.25 mmol fructose)	Au/HT (0.25 g), water (10 mL), Na_2CO_3 (1 mmol)	95 °C ,7 h	55	0.393	**23**
Fructose derived HMF (7.5 wt %)	Pt/C (5 wt %, 0.25 g), GVL/water (5 mL)	110 °C, 16 h	93	0.122	**24**
Fructose (10 g/L)	PtBi/C (0.375 g), MIBK (50 mL)	80 °C, 70 h	25	0.026	**25**
Fructose-derived HMF (0.63 wt %)	Pt/C (0.2 g), K_2CO_3 (0.276 g), water/DMSO (20g)	100 °C, 10 h	78	0.39	**26**
Glucose (converted to 0.68 mmol HMF)	Au/HT (2.142 mg), water (10 mL)	95 °C, 6 h	77.9	41.217	**27**
Hardwood chips (converted to 0.74 mmol HMF)	Au/HT (2.331 mg), water (10 mL)	95 °C, 6 h	25.7	13.598	**27**
Hardwood chips (converted to 1.01 mmol HMF)	Au/HT (3.1815 mg), water (10 mL)	95 °C, 6 h	65.3	34.551	**27**
Fructose (0.1 mmol)	Fe–Zr–O (0.01 g), [Bmim]Cl (1g)	160 °C, 24 h	46.4	0.193	**28**
Fructose (0.5 mmol)	$ZnFe_{1.65}Ru_{0.35}O_4$ (100 mg), DMSO (3 mL)	130 °C, 16 h	91.2	0.285	**29**
Fructose (100 mg)	nano-Fe_3O_4–CoO_x (100 mg), DMSO (4 mL)	80 °C, 15 h	59.8	0.221	**30**
Fructose (0.1 g)	$Co(acac)_3$-gel (0.05 g), water (6 mL)	160 °C, 65 min	70	7.179	**31**
HMF (0.25 mmol)	Co-Mn mixed oxide (50 mg), $NaHCO_3$ (0.5 mmol), water (5 mL)	120 °C, 5 h	95	0.95	**32**
HMF (17.65 mmol)	MnO_2 (10 g), $NaHCO_3$ (3.02 g), water (90 mL)	100 °C, 24 h	86 (2.36 g)	0.063	**10**

HMF (2 mmol)	Ru(4%)/$MnCo_2O_4$ (0.2 g), water (20 mL)	120 °C, 10 h	99.1	0.991	**33**
HMF (0.126 g)	Ni–MnOx (0.1 g), $NaHCO_3$ (0.336 g), H_2O (10 mL)	100 °C, 28 h	93.8	0.335	**34**
HMF (50 mmol)	Mn_2O_3 nanoflakes (150 mg), $NaHCO_3$ (3 equiv.), water (20 mL)	100 °C, 24 h	>99	13.889	**35**
Rice straw (1.9 g, having 36.6 % cellulose)	MnO_2 (0.55 g)	192.5°C, 34 min	52.1	7.176	**36**
HMF (0.794 mmol)	Mn_1Fe_1 (2.5 mg/mL), GVL-water (10 mL)	3 h ozone, 130 °C, 2 h heating	60	6.349	**37**
Whey permeate powder (equiv. to 1.2 mmol lactose)	Mn_1Fe_1 (2.5 mg/mL), GVL-water (10 mL)	3 h ozone, 130 °C, 2 h heating	14.6	1.402	**37**
HMF (1 mmol)	$Fe_1Co_1Ni_1Cu_1Ga_1Pt_2$/C（0.2 g）-water (20 mL)	4 h, 100 °C，0.5 MPa O_2	98.6	1.248	This work

10. DFT study

Table S5 The average Bader charge transfer in electron kind atom in HEA (High Entropy Alloy) model

Entry	Atom	Bader charge / e
1	Pt	0.72
2	Fe	-0.37
3	Co	-0.10
4	Ni	0.06
5	Cu	0.00
6	Ga	-0.32

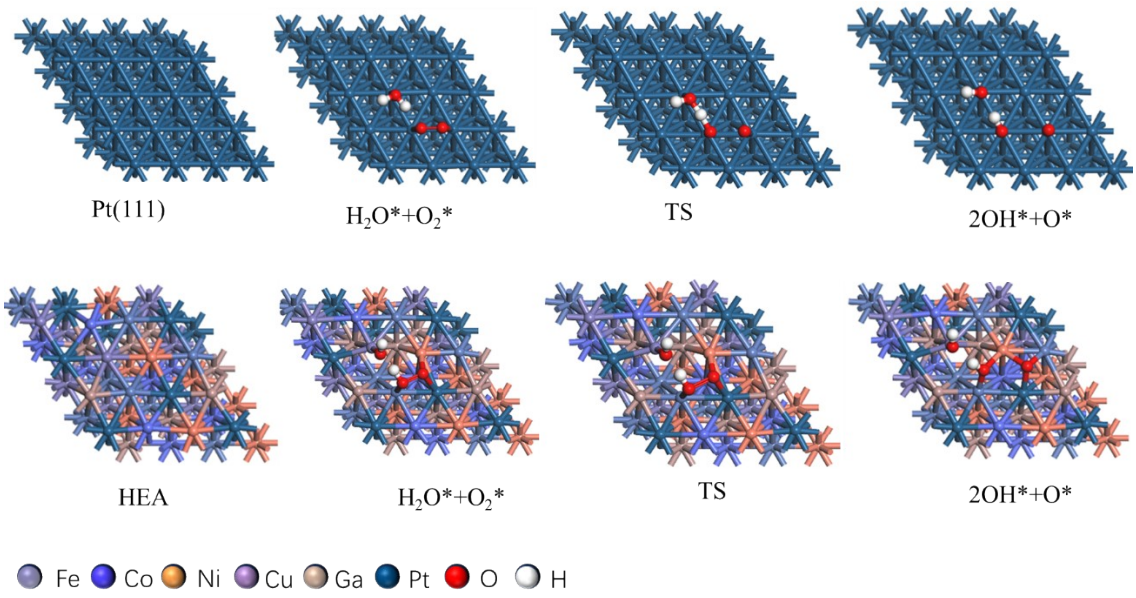

Figure S7. The optimal adsorption activation model for O_2 molecules on Pt (111) and HEA (111) surfaces in the presence of water

References:

1. Cao, G.; Liang, J.; Guo, Z.; Yang, K.; Wang, G.; Wang, H.; Wan, X.; Li, Z.; Bai, Y.; Zhang, Y.; Liu, J.; Feng, Y.; Zheng, Z.; Lu, C.; He, G.; Xiong, Z.; Liu, Z.; Chen, S.; Guo, Y.; Zeng, M.; Lin, J.; Fu, L., Liquid metal for high-entropy alloy nanoparticles synthesis. *Nature* **2023**.
2. Yao, L.; Zhang, F.; Yang, S.; Zhang, H.; Li, Y.; Yang, C.; Yang, H.; Cheng, Q., Sub-2 nm IrRuNiMoCo High-Entropy Alloy with Iridium-Rich Medium-Entropy Oxide Shell to Boost Acidic Oxygen Evolution. *Advanced Materials* **2024,** *36* (25).
3. Feng, G.; Ning, F.; Song, J.; Shang, H.; Zhang, K.; Ding, Z.; Gao, P.; Chu, W.; Xia, D., Sub-2 nm Ultrasmall High-Entropy Alloy Nanoparticles for Extremely Superior Electrocatalytic Hydrogen Evolution. *J. Am. Chem. Soc.* **2021,** *143* (41), 17117-17127.
4. Yifan Sun, S. D., High-entropy materials for catalysis: A new frontier. **2021**.
5. Yao, Y.; Huang, Z.; Hughes, L. A.; Gao, J.; Li, T.; Morris, D.; Zeltmann, S. E.; Savitzky, B. H.; Ophus, C.; Finfrock, Y. Z.; Dong, Q.; Jiao, M.; Mao, Y.; Chi, M.; Zhang, P.; Li, J.; Minor, A. M.; Shahbazian-Yassar, R.; Hu, L., Extreme mixing in nanoscale transition metal alloys. *Matter* **2021,** *4* (7), 2340-2353.
6. Liang, J.; Cao, G.; Zeng, M.; Fu, L., Controllable synthesis of high-entropy alloys. *Chem. Soc. Rev.* **2024**.
7. Gao, Z.; Li, C.; Fan, G.; Yang, L.; Li, F., Nitrogen-doped carbon-decorated copper catalyst for highly efficient transfer hydrogenolysis of 5-hydroxymethylfurfural to convertibly produce 2,5-dimethylfuran or 2,5-dimethyltetrahydrofuran. *Appl. Catal. B: Environ.* **2018,** *226*, 523-533.
8. Wang, Q.; Hou, W.; Li, S.; Xie, J.; Li, J.; Zhou, Y.; Wang, J., Hydrophilic mesoporous poly(ionic liquid)-supported Au–Pd alloy nanoparticles towards aerobic oxidation of 5-hydroxymethylfurfural to 2,5-furandicarboxylic acid under mild conditions. *Green Chem.* **2017,** *19* (16), 3820-3830.
9. Luo, J.; Wei, H.; Liu, Y.; Zhang, D.; Zhang, B.; Chu, W.; Pham-Huu, C.; Su, D. S., Oxygenated group and structural defect enriched carbon nanotubes for immobilizing gold nanoparticles. *Chem Commun (Camb)* **2017,** *53* (95), 12750-12753.
10. Hayashi, E.; Komanoya, T.; Kamata, K.; Hara, M., Heterogeneously-Catalyzed Aerobic Oxidation of 5-Hydroxymethylfurfural to 2,5-Furandicarboxylic Acid with MnO2. *ChemSusChem* **2017,** *10* (4), 654-658.
11. Gupta, K.; Rai, R. K.; Dwivedi, A. D.; Singh, S. K., Catalytic Aerial Oxidation of Biomass-Derived Furans to Furan Carboxylic Acids in Water over Bimetallic Nickel-Palladium Alloy Nanoparticles. *ChemCatChem* **2017,** *9* (14), 2760-2767.
12. Gong, W.; Zheng, K.; Ji, P., Platinum deposited on cerium coordination polymer for catalytic oxidation of hydroxymethylfurfural producing 2,5-furandicarboxylic acid. *RSC Advances* **2017,** *7* (55), 34776-34782.
13. Donoeva, B.; Masoud, N.; de Jongh, P. E., Carbon Support Surface Effects in the Gold-Catalyzed Oxidation of 5-Hydroxymethylfurfural. *ACS Catal.* **2017,** *7* (7), 4581-4591.
14. Chen, C.; Li, X.; Wang, L.; Liang, T.; Wang, L.; Zhang, Y.; Zhang, J., Highly Porous Nitrogen- and Phosphorus-Codoped Graphene: An Outstanding Support for Pd Catalysts to Oxidize 5-Hydroxymethylfurfural into 2,5-Furandicarboxylic Acid. *ACS Sustain. Chem. Eng.* **2017,** *5* (12), 11300-11306.
15. Gui, Z.; Cao, W.; Saravanamurugan, S.; Riisager, A.; Chen, L.; Qi, Z., Efficient Aerobic Oxidation of 5-Hydroxymethylfurfural in Aqueous Media with Au-Pd Supported on Zinc

Hydroxycarbonate. *ChemCatChem* **2016,** *8* (23), 3636-3643.
16. Zhou, C.; Deng, W.; Wan, X.; Zhang, Q.; Yang, Y.; Wang, Y., Functionalized Carbon Nanotubes for Biomass Conversion: The Base-Free Aerobic Oxidation of 5-Hydroxymethylfurfural to 2,5-Furandicarboxylic Acid over Platinum Supported on a Carbon Nanotube Catalyst. *ChemCatChem* **2015,** *7* (18), 2853-2863.
17. Albonetti, S.; Lolli, A.; Morandi, V.; Migliori, A.; Lucarelli, C.; Cavani, F., Conversion of 5-hydroxymethylfurfural to 2,5-furandicarboxylic acid over Au-based catalysts: Optimization of active phase and metal–support interaction. *Appl. Catal. B: Environ.* **2015,** *163*, 520-530.
18. Albonetti, S.; Pasini, T.; Lolli, A.; Blosi, M.; Piccinini, M.; Dimitratos, N.; Lopez-Sanchez, J. A.; Morgan, D. J.; Carley, A. F.; Hutchings, G. J.; Cavani, F., Selective oxidation of 5-hydroxymethyl-2-furfural over TiO2-supported gold–copper catalysts prepared from preformed nanoparticles: Effect of Au/Cu ratio. *Catal. Today* **2012,** *195* (1), 120-126.
19. Davis, S. E.; Houk, L. R.; Tamargo, E. C.; Datye, A. K.; Davis, R. J., Oxidation of 5-hydroxymethylfurfural over supported Pt, Pd and Au catalysts. *Catal. Today* **2011,** *160* (1), 55-60.
20. Yi, G.; Teong, S. P.; Zhang, Y., The Direct Conversion of Sugars into 2,5-Furandicarboxylic Acid in a Triphasic System. *ChemSusChem* **2015,** *8* (7), 1151-1155.
21. Schade, O. R.; Dannecker, P.-K.; Kalz, K. F.; Steinbach, D.; Meier, M. A. R.; Grunwaldt, J.-D., Direct Catalytic Route to Biomass-Derived 2,5-Furandicarboxylic Acid and Its Use as Monomer in a Multicomponent Polymerization. *ACS Omega* **2019,** *4* (16), 16972-16979.
22. Rathod, P. V.; Jadhav, V. H., Efficient Method for Synthesis of 2,5-Furandicarboxylic Acid from 5-Hydroxymethylfurfural and Fructose Using Pd/CC Catalyst under Aqueous Conditions. *ACS Sustain. Chem. Eng.* **2018,** *6* (5), 5766-5771.
23. Yi, G.; Teong, S. P.; Li, X.; Zhang, Y., Purification of Biomass-Derived 5-Hydroxymethylfurfural and Its Catalytic Conversion to 2,5-Furandicarboxylic Acid. *ChemSusChem* **2014,** *7* (8), 2131-2135.
24. Motagamwala, A. H.; Won, W.; Sener, C.; Alonso, D. M.; Maravelias, C. T.; Dumesic, J. A., Toward biomass-derived renewable plastics: Production of 2,5-furandicarboxylic acid from fructose. *Sci. Adv.* **2018,** *4* (1).
25. Kr¨, M.; oger, U. P.; Vorlop, u. a. K.-D., A new approach for the production of 2,5-furandicarboxylic acid by in situ oxidation of 5-hydroxymethylfurfural starting from fructose. *Top. Catal.* **2000,** *13*, 237-242.
26. Chen, G.; Wu, L.; Fan, H.; Li, B.-g., Highly Efficient Two-Step Synthesis of 2,5-Furandicarboxylic Acid from Fructose without 5-Hydroxymethylfurfural (HMF) Separation: In Situ Oxidation of HMF in Alkaline Aqueous H2O/DMSO Mixed Solvent under Mild Conditions. *Industrial & Engineering Chemistry Research* **2018,** *57* (48), 16172-16181.
27. Liu, L.; Chang, H.-m.; Jameel, H.; Park, J.-Y.; Park, S., Catalytic Conversion of Biomass Hydrolysate into 5-Hydroxymethylfurfural. *Industrial & Engineering Chemistry Research* **2017,** *56* (49), 14447-14453.
28. Yan, D.; Wang, G.; Gao, K.; Lu, X.; Xin, J.; Zhang, S., One-Pot Synthesis of 2,5-Furandicarboxylic Acid from Fructose in Ionic Liquids. *Industrial & Engineering Chemistry Research* **2018,** *57* (6), 1851-1858.
29. Yang, Z.; Qi, W.; Su, R.; He, Z., Selective Synthesis of 2,5-Diformylfuran and 2,5-Furandicarboxylic Acid from 5-Hydroxymethylfurfural and Fructose Catalyzed by Magnetically Separable Catalysts. *Energy & Fuels* **2016,** *31* (1), 533-541.
30. Wang, S.; Zhang, Z.; Liu, B., Catalytic Conversion of Fructose and 5-Hydroxymethylfurfural into

2,5-Furandicarboxylic Acid over a Recyclable Fe3O4–CoOxMagnetite Nanocatalyst. *ACS Sustain. Chem. Eng.* **2015,** *3* (3), 406-412.
31. Ribeiro, M. L.; Schuchardt, U., Cooperative effect of cobalt acetylacetonate and silica in the catalytic cyclization and oxidation of fructose to 2,5-furandicarboxylic acid. *Catalysis Communications* **2003,** *4* (2), 83-86.
32. Rao, K. T. V.; Rogers, J. L.; Souzanchi, S.; Dessbesell, L.; Ray, M. B.; Xu, C., Inexpensive but Highly Efficient Co–Mn Mixed-Oxide Catalysts for Selective Oxidation of 5-Hydroxymethylfurfural to 2,5-Furandicarboxylic Acid. *ChemSusChem* **2018,** *11* (18), 3323-3334.
33. Mishra, D. K.; Lee, H. J.; Kim, J.; Lee, H.-S.; Cho, J. K.; Suh, Y.-W.; Yi, Y.; Kim, Y. J., MnCo2O4 spinel supported ruthenium catalyst for air-oxidation of HMF to FDCA under aqueous phase and base-free conditions. *Green Chem.* **2017,** *19* (7), 1619-1623.
34. Yu, K.; Liu, Y.; Lei, D.; Jiang, Y.; Wang, Y.; Feng, Y.; Lou, L.-L.; Liu, S.; Zhou, W., M3+O(–Mn4+)2 clusters in doped MnOx catalysts as promoted active sites for the aerobic oxidation of 5-hydroxymethylfurfural. *Catal. Sci. Technol.* **2018,** *8* (9), 2299-2303.
35. Bao, L.; Sun, F. Z.; Zhang, G. Y.; Hu, T. L., Aerobic Oxidation of 5-Hydroxymethylfurfural to 2,5-Furandicarboxylic Acid over Holey 2 D Mn2 O3 Nanoflakes from a Mn-based MOF. *ChemSusChem* **2020,** *13* (3), 548-555.
36. Chai, Y.; Yang, H.; Bai, M.; Chen, A.; Peng, L.; Yan, B.; Zhao, D.; Qin, P.; Peng, C.; Wang, X., Direct production of 2, 5-Furandicarboxylicacid from raw biomass by manganese dioxide catalysis cooperated with ultrasonic-assisted diluted acid pretreatment. *Bioresource Technology* **2021,** *337*, 125421.
37. Yang, Z.-Y.; Wen, M.; Zong, M.-H.; Li, N., Synergistic chemo/biocatalytic synthesis of 2,5-furandicarboxylic acid from 5-hydroxymethylfurfural. *Catalysis Communications* **2020,** *139*, 105979.